FE/LE and Spatial Variability Analysis of Basal Heave Stability for Excavations Supported by Diaphragm Walls

Anthony T.C. Goh[1], R.H. Zhang[2], W.G. Zhang[3], and K.S. Wong[4]

[1]School of Civil & Environmental Engrg., Nanyang Technological University, Nanyang Avenue, Singapore 639798. E-mail: ctcgoh@ntu.edu.sg
[2]School of Civil Engineering, Chongqing University, Chongqing, China 400045. E-mail: zhangrh@cqu.edu.cn
[3]School of Civil Engineering, Chongqing University, Chongqing, China 400045. E-mail: cheungwg@126.com/zhangwg@ntu.edu.sg
[4]WKS Geotechnical Consultants, 60 Kallang Pudding Road, Singapore 349320. Email: wongks@gmail.com

Abstract: Flexible sheetpile walls and stiff diaphragm walls are commonly used as support systems for excavations in deep deposits of soft clays. While a number of numerical studies have shown that there is a general trend of decreasing wall movements with increasing wall stiffness particularly when the basal heave factor of safety is low, only limited studies have been carried out to assess the effects of using a stiff retaining wall system such as diaphragm walls on the factor of safety against basal heave. In this paper, the assessment of basal heave instability for deep excavations in soft clay using nonlinear finite element analyses is considered for a number of cases with different geometrical properties of the excavation, wall and soil properties. The study indicated that the increase in the basal heave factor of safety with increasing wall penetration depth is more significant for diaphragm walls compared with sheetpile walls. The finite element analyses also highlight that the depth to the hard stratum from the tip of the wall is a key component of the resistance of the excavation system to basal heave failure. Subsequently, a comparative study of the basal heave factor of safety predicted by the finite element analysis with the modified Terzaghi method was carried out. Subsequently, reliability analyses that considered the spatial variability of the soft clay were performed and some useful conclusions regarding the effects of spatial averaging as well as the coefficient of variation of the soil properties are presented.

Keywords: Basal heave; braced excavation; clay; diaphragm wall; factor of safety.

1 Introduction

In built-up urban environments, the construction of underground infrastructure is increasingly being considered to optimize land use. In areas with deep deposits of soft clays, the use of braced excavation systems is the generally preferred construction option. The design of braced excavation in soft clays involves the assessment of: (i) the basal heave stability of the excavation during construction, (ii) the structural capacity of the struts, walers and retaining walls, and (iii) the serviceability issues related to excessive wall and ground movements. While a number of studies of braced excavations in soft clays (e.g., Mana and Clough 1981; Clough et al. 1989; Wong and Broms 1989; Moorman 2004; Kung et al. 2007; Bryson and Zapata-Medina 2012) have shown that there is a general trend of decreasing wall movements with increasing wall stiffness particularly when the basal heave factor of safety is low, only limited finite element (FE) studies (Goh 1994; Faheem et al. 2003; Faheem et al. 2004) have been carried out to examine the effects of using stiff retaining walls systems such as diaphragm walls and secant bored piles on the basal heave factor of safety. In these previous studies, various geometrical properties of the excavation and wall properties were varied and the stability of the excavation was assessed using the shear strength reduction technique (Zienkiewicz et al. 1975). The general conclusion from these numerical studies was that the basal heave factor of safety increases with increasing wall stiffness mainly because of the reduced tendency of the soft clay to displace towards the excavation.

One of the aims of this paper is to carry out a comparative study of the basal heave factor of safety predictions for diaphragm walls using FE method with the predictions using the modified Terzaghi method. The effects of penetration depth, excavation width, as well as the depth to the hard stratum from the tip of the wall on the factor of safety for sheetpile and diaphragm walls were examined respectively. The validity of the modified Terzaghi method that considers the diaphragm wall penetration depth and depth to the hard stratum is confirmed to give predictions that are consistent with the basal heave factor of safety obtained from the FE analyses.

2 Modified Terzaghi Method

The modified Terzaghi method (Wong and Goh 2002; Goh et al. 2008) is commonly used to assess the basal heave factor of safety for excavations with stiff diaphragm walls. In this method, following the assumption

Proceedings of the 7th International Symposium on Geotechnical Safety and Risk (ISGSR)
Editors: Jianye Ching, Dian-Qing Li and Jie Zhang

Published by Research Publishing, Singapore.
ISBN: 978-981-11-2725-0; doi:10.3850/978-981-11-2725-0_IS9-16-cd

adopted by Eide et al. (1972), the failure is assumed to occur beneath the base of the wall and is partially resisted by the interior wall adhesion $f_s = \alpha c_u$, as illustrated in Fig. 1, in which α is the clay-wall adhesion factor. The α value typically varies between 0.5 for stiff clays to 1.0 for soft clays (NAVFAC DM7.2 1986). The factor of safety FS_{DW} can be expressed as:

$$FS_{DW} = \frac{N_c c_{ub} B_1 + c_{uh} H + c_{ud} D + f_s D}{(\gamma H + q) B_1} \quad (1)$$

As illustrated in Fig 1, γ is the unit weight of the soil, c_{uh} is the undrained shear strength of the clay from the ground surface to the final depth of excavation H, c_{ud} is the undrained shear strength of the clay from depth H to the tip of the wall, and c_{ub} is the undrained shear strength of the clay below the final excavation level.

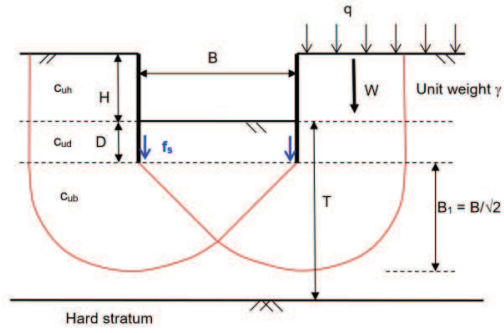

Figure 1. Modified Terzaghi method for basal heave stability for diaphragm walls.

3 Finite Element Analyses

In this study, extensive plane strain FE analyses were carried out to assess the basal heave factor of safety for wide excavations in clay. The parametric study was performed using the FE software Plaxis (Brinkgreve et al. 2016). The soil was modeled by 15-noded triangular elements, with the Mohr-Coulomb failure criterion. The wall structural elements were assumed to be linear elastic and were modeled by 5-noded beam elements. The interface elements that model the slippage between the soil and the wall consist of 10-noded joint elements. The shear response of the interface element is controlled by an elastic–perfectly plastic Coulomb shear strength criterion. The struts (not shown in Fig. 4) were modeled by linear elastic 3-noded bar elements. The nodes along the side boundaries of the mesh were constrained from displacing horizontally while the nodes along the bottom boundary were constrained from moving horizontally and vertically. The right vertical boundary extends far from the excavation (~5B) to minimize the effects of the boundary restraints. The input parameters for the elastic-plastic Mohr-Coulomb constitutive relationship are the undrained elastic modulus E_u, the undrained Poisson's ratio υ_u, the undrained friction angle ϕ_u, the dilation angle ψ and the undrained cohesion c_u. For this study, cases with a homogeneous clay layer with constant undrained shear strength c_u and also cases with c_u increasing linearly with depth were considered. The soil is assumed to be subjected to undrained shearing during excavation. Only clays with isotropic c_u are considered. A total of 104 different cases were analyzed. The parameters that were varied include the undrained shear strength c_u, the width of the excavation B, the depth of the excavation H, the wall penetration depth D, the depth to the hard stratum T, and the wall stiffness EI. The range of soil, wall and geometrical properties of the excavation that were analyzed are shown in Table 1.

The construction sequence comprised the following steps: (1) the wall is installed ("wished into place") without any disturbance in the surrounding soil; (2) the soil is excavated uniformly in 2 m intervals, and struts are installed until the final depth H is reached. The stability of the excavation was then determined using the shear strength reduction technique.

4 Finite Element Results

The general trends of the FE analyses are highlighted in this section. Analyses with different wall thickness from 0.6 m to 1.2 m showed minimal differences in FS_{FE}. For brevity, these results have been omitted. In all the plots in this paper, only the results with 1.2 m thick diaphragm walls (EI = 4.032×10^6 kNm^2/m) are shown. Figure 2(a) shows a typical plot of the plastic points at the end of excavation to the final excavation level for H = 16 m with B = 20 m and D = 16 m. Figure 2(b) shows the corresponding deformed mesh (at an exaggerated scale) after the shear strength reduction phase. The plots show a "block" type vertical movement the soil beneath the excavation

and the contribution of the shear resistance between the wall and the soil to resist basal heave instability for diaphragm walls. Figure 2(c) plots the phase displacement for c-phi reduction phase.

Table 1. Summary of soil, structural and geometrical properties.

Parameter	Range of values
Geometrical, wall and strut properties	
Excavation width B (m)	20 – 100
Excavation depth H (m)	16 – 24
Depth of wall penetration D (m)	4 – 24
Depth to hard stratum T (m)	10 – 120
Wall stiffness EI (kNm^2/m)	8.364×10^3 – 4.032×10^6
Strut axial stiffness EA (kN/m)	2.0×10^6
Soil properties	
Soil unit weight γ (kN/m^3)	16
Soil undrained shear strength c_u (kPa)*	35 – 100
c_{u0} (kPa)$^{\#}$	5 - 10
m (kPa/m)$^{\#}$	1 – 1.5
Soil elastic modulus ratio E_u/c_u	300
Poisson's ratio υ_u	0.495
Friction angle ϕ_u (degrees)	0
Dilation angle ψ (degrees)	0
Clay-wall adhesion factor α	0.5 – 1.0

* constant c_u

$^{\#}c_u$ linearly increasing with depth from the ground surface $z = c_{u0}+mz$ (kPa)

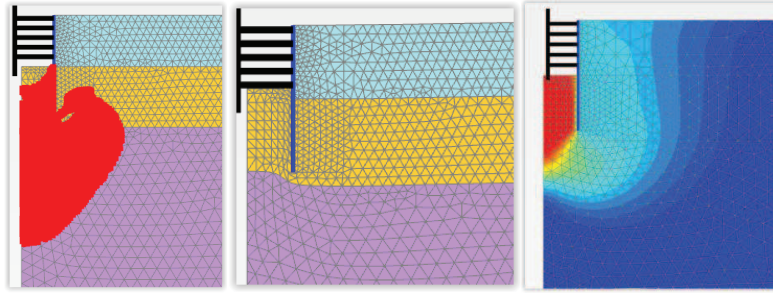

Figure 2. (a) Plastic points after excavation to H = 16 m, (b) Deformed mesh after shear strength reduction analyses for H = 16 m, (c) phase displacement for c-phi reduction.

The influence of the width of the excavation B and the wall penetration depth D on FS_{FE} is shown in Figure 3. For comparison, the results for a flexible sheetpile wall (EI = 8,364 kNm^2/m) are also shown. For both the sheetpile wall and diaphragm wall, the basal heave factor of safety FS_{FE} decreases with the increase of the excavation width. For the sheetpile wall, the increase of the wall penetration depth D from 4 m to 8 m results in a slight increase in FS_{FE}. However, subsequent increases in D result in minimal increases in FS_{FE}, which indicates a critical embedded length for flexible walls. The influence of D on FS_{FE} is more significant for the rigid diaphragm wall. For example, for the case with B = 30 m, the FS_{FE} increased by 31% when D was increased from 4 m to 24 m. The general conclusion from these numerical studies was that the basal heave factor of safety increases with increasing wall stiffness mainly because of the reduced tendency of the soft clay to displace towards the excavation.

Figure 4 shows the influence of the depth from the wall tip to the hard stratum (T – D) on the factor of safety. As expected, the presence of the hard stratum close to the excavation significantly increases the FS_{FE}. The factor of safety increases significantly for (T - D)/B < 0.7 as the hard stratum prevents the full development of the failure surface of the soil, just as in the case of the ultimate bearing capacity of a footing with a rigid base at shallow depth (Chen 1975). For example, for the case with D = 8 m, the FS_{FE} = 1.31 for (T - D)/B = 1.8 compared with FS_{FE} = 1.57 for (T – D)/B = 0.3. The results also highlight that for the same (T – D)/B ratio, increasing D will have an influence on the factor of safety. It can be concluded that the thickness of the clay beneath the wall tip (T – D) is a key component of the resistance of the excavation system to basal heave failure.

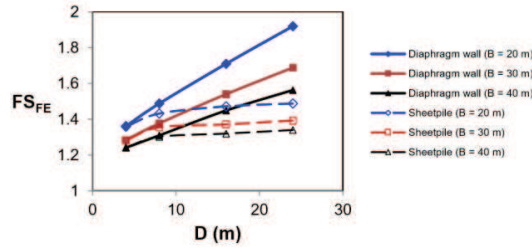

Figure 3. Effects of excavation width B and wall penetration D on FS_{FE} (H = 16 m, T = 100 m and c_u = 50 kPa).

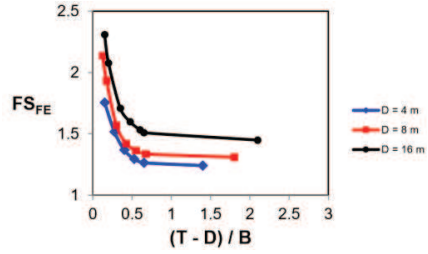

Figure 4. Effects of (T – D)/B on FS_{FE} (B = 40 m, H = 16 m, and c_u = 50 kPa).

5 Comparison between FE and Limit Equilibrium Methods

In order to account for the influence of the hard stratum at a shallow depth, based on regression analysis of the FE results, the bearing capacity factor N_c in Eq. (1) has been modified as shown in Figure 5 and Eq. (2). The proposed N_c values are in good agreement with the upper bound N_c values proposed by Chen (1975) for calculating the bearing capacity of a soft clay overlying a strong clay layer as shown in Figure 5.

$$N_c = -21.6[(T\text{-}D)/B]^3 + 42.2[(T\text{-}D)/B]^2 - 28.8[(T\text{-}D)/B] + 12.6 \quad \textit{for } (T\text{-}D)/B \le 0.7$$
$$N_c = 5.7 \quad \textit{for } (T\text{-}D)/B > 0.7 \qquad (2)$$

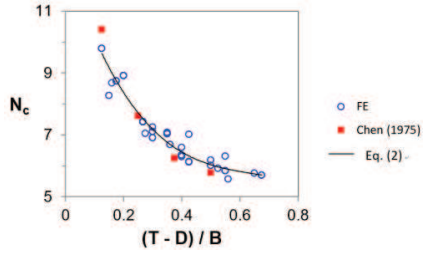

Figure 5. N_c values for (T-D)/B ≤ 0.7.

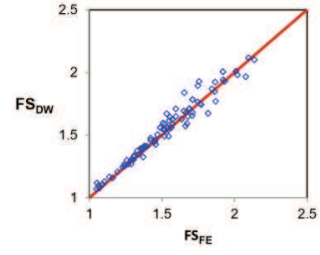

Figure 6. Comparison of FS_{DW} versus FS_{FE}.

Figure 6 shows the plot of FS_{DW} obtained using Eqs. (1) and (2) versus the FS_{FE} values for all the diaphragm wall cases is reasonably accurate. The mean and COV for the ratio FS_{DW}/FS_{FE} are 1.03 and 0.03, respectively. In this study, clays with constant c_u as well as clays with c_u increasing linearly with depth were also considered. For clays with c_u increasing linearly with depth, the average c_u values were used. For example, the c_{uh} value is taken as the average c_u from the ground surface to the depth H, and the c_{ub} value is taken as the average c_u from depth H to depth $(H + B_1)$ in which $B_1 = B/\sqrt{2}$.

6 Spatial Variability Analysis

Figure 7 shows the spreadsheet setup for evaluating the spatial variability reliability index β for the modified Terzaghi expression in Eq. (1). This spreadsheet is modified from the original version by Goh et al. (2008) by introducing the spatial factors as shown in Cells B21:C24. The eight lognormally distributed and uncorrelated variables are c_{ub}, c_{uh}, q, γ, H, c_{ud}, f_s, and D. The width of the excavation B = 20 m, is assumed to be constant in the analysis. The uncertainties in the parameters H and D could arise from construction deviations in the actual excavation depth and depth of wall penetration, respectively.

4		B	20		Modified Terzaghi															
5																				
6			x value	mean	SD	cov					[nx]		Correlation matrix [R]							
7		c_{ub} (kPa)	40.94774	50	10	0.2					-1.07223		1	0	0	0	0	0	0	0
8		c_{uh} (kPa)	46.42352	50	10	0.2					-0.28124		0	1	0	0	0	0	0	0
9		q (kPa/m)	9.91266	10	2	0.2					0.053067		0	0	1	0	0	0	0	0
10		γ (kN/m^3)	18.95519	16	2.4	0.15					1.223219		0	0	0	1	0	0	0	0
11		H (m)	16.00388	16	0.1	0.00625					0.042303		0	0	0	0	1	0	0	0
12		c_{ud} (kPa)	48.35338	50	10	0.2					-0.07318		0	0	0	0	0	1	0	0
13		fs (kPa)	48.35338	50	10	0.2					-0.07318		0	0	0	0	0	0	1	0
14		D (m)	3.996955	4	0.1	0.025					-0.01846		0	0	0	0	0	0	0	1
15																				
16																				
17			transpose [nx]										inverse [R]							
18																				
19		-1.0722298	-0.28124	0.053067384	1.223219	0.042303	-0.07318	-0.07318	-0.01846				1	0	0	0	0	0	0	0
20													0	1	0	0	0	0	0	0
21		Spatial factors									[R]$^{-1}$[nx]		0	0	1	0	0	0	0	0
22		θ (m)	50										0	0	0	1	0	0	0	0
23		L (m)	27								-1.07223		0	0	0	0	1	0	0	0
24		Γ	0.848216								-0.28124		0	0	0	0	0	1	0	0
25											0.053067		0	0	0	0	0	0	1	0
26											1.223219		0	0	0	0	0	0	0	1
27											0.042303									
28			Invoke Solver to minimize β								-0.07318									
29			by changing x values								-0.07318									
30											-0.01846									
31			subject to G(x) = 0											FS$_{limit}$	1					
32																				
33				β							[nx]^{T}R^{-1}[nx]									
34				1.655504914							2.740697			G(x)	-4.87208E-07					
35																				
36				β = sqrt of {[nx]^{T}R^{-1}[nx]}										G(x) = FS - FS$_{limit}$						

Figure 7. Spreadsheet setup for evaluating the reliability index considering spatial variability.

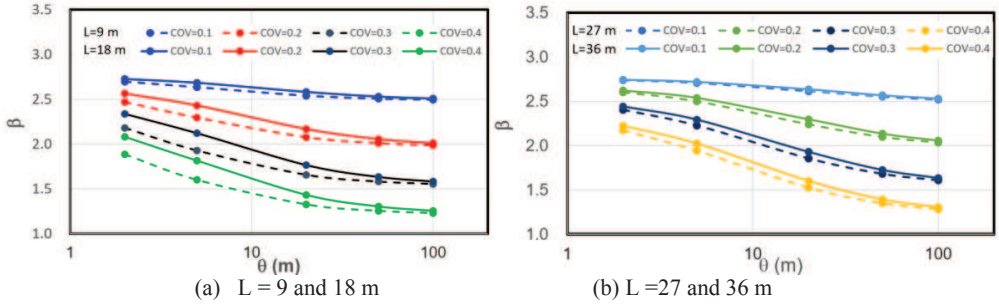

(a) L = 9 and 18 m (b) L =27 and 36 m

Figure 8. Influence of COV of c_{ub} and characteristic length L.

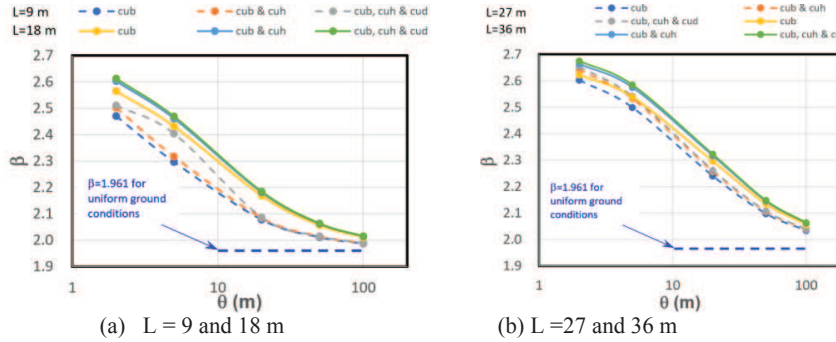

(a) L = 9 and 18 m (b) L =27 and 36 m

Figure 9. Effects of soil layers considering spatial variability.

Figures 8a and b show the effects of COV of c_{ub} and characteristic length L on the reliability index β. It is obvious that for the same θ, β decreases as the COV of c_{ub} increases, and greater characteristic length results in slightly larger β values.

Figure 9a shows the effects of different combinations of spatial variability of c_u of the soil layers for L = 9 and 18 m, respectively. Also shown is the case without considering the spatial variability. It is obvious that as the scale of fluctuation increases, which indicates an increasing uniform ground, the reliability index β values considering spatial variability converge to the constant value of 1.961. The plot shows that when only the spatial variability of c_{ub} is considered, β is slightly lower than when combinations of c_{ub} & c_{uh}, as well as c_{ub}, c_{uh} & c_{ud} are considered. This again suggests that the design can be too conservative if the effects of spatial variability of the soil parameters are not considered. Fig. 9b which shows the spatial variability effects for L =27 and 36 m, respectively, display similar trends as with Fig. 9a with slightly larger β for the same θ.

7 Summary and Conclusions

FE analyses were carried out to assess the basal heave factor of safety for excavations in soft clays supported by diaphragm walls. A total of 104 different cases with different geometrical properties of the excavation, wall and soil properties were considered. Comparing the factor of safety for sheetpile and diaphragm walls, the increase in FS_{FE} with increasing D is more significant for diaphragm walls. The basal heave factor of safety FS_{FE} was found to decrease with the increase of the excavation width. The FE analyses also highlight that the depth to the hard stratum from the tip of the wall is a key component of the resistance of the excavation system to basal heave failure.

The validity of the modified Terzaghi method in Eqs. (1) and (2) that considers the wall penetration depth and depth to the hard stratum for diaphragm walls is confirmed to give predictions that are consistent with the basal heave factor of safety obtained from FE analyses. Consideration of the spatial variability would generally result in a higher reliability index. Conventional analysis assuming uniform ground conditions generally results in a more conservative design. Parametric analyses show the reliability index is significantly influenced by various factors such as the spatial variability of the different soil layers, the scale of fluctuation, the characteristic length, and the COV of c_{ub}.

Acknowledgments

The corresponding author is grateful to the financial support from the National Natural Science Foundation of China (51608071), the Venture & Innovation Support Program for Chongqing Overseas Returnees (cx2017123), Special Funding for Postdoctoral research projects in Chongqing (Xm2017007) and the sponsorship by Natural Science Foundation of Chongqing, China (cstc2018jcyjAX0632).

References

Brinkgreve L.B.J, Kumarswamy S., and Swolfs W.M. (2016). *Plaxis 2D User Manual*, PLAXIS BV, Netherlands.

Bryson L. and Zapata-Medina D. (2012). Method for estimating system stiffness for excavation support walls. *Journal of Geotechnical and Geoenvironmental Engineering*, 138(9), 1104-1115.

Chen W.F. (1975). *Limit Analyses and Soil Plasticity*, Elsevier, Amsterdam, Netherlands.

Clough G.W., Smith E.M., and Sweeney B.P. (1989). Movement control of excavation support systems by iterative design. *Proc. Foundation Engineering Congress on Current Principles and Practices*, Evanston, USA, 2, 869–884.

Eide O., Aas G., and Josang T. (1972). *Special Applications of Cast-In-Place Walls for Tunnels in Soft Clay in Oslo*, Norwegian Geotechnical Institute, Oslo, 91, 63-72.

Faheem H., Cai F., Ugai K., and Hagiwara T. (2003). Two-dimensional base stability of excavations in soft soils using FEM. *Computers and Geotechnics*, 30(2), 141-163.

Faheem H., Cai F., and Ugai, K. (2004). Three-dimensional base stability of rectangular excavations in soft soils using FEM. *Computers and Geotechnics*, 31(2), 67-74.

Goh A.T.C. (1994). Estimating basal heave stability for braced excavations in soft clay. *Journal of Geotechnical and Geoenvironmental Engineering*, 120(8), 1430-1436.

Goh A.T.C, Kulhawy F.H., and Wong K.S. (2008). Reliability assessment of basal-heave stability for braced excavations in clay. *Journal of Geotechnical and Geoenvironmental Engineering*, 134(2), 145-153.

Kung G.T.C, Juang C.H., Hsiao E.C.L., and Hashash Y.M.A. (2007). Simplified model for wall deflection and ground-surface settlement caused by braced excavation in clays. *Journal of Geotechnical and Geoenvironmental Engineering*, 133(6), 731–747.

Mana A.I. and Clough G.W. (1981). Prediction of movement for braced cuts in clay. *Journal of Geotechnical and Geoenvironmental Engineering*, 107(6), 759–777.

Moormann C. (2004). Analysis of wall and ground movements due to deep excavations in soft soil based on a new worldwide database. *Soils and Foundations*, 44(1), 87-98.

NAVFAC, DM-7.2 (1986). *Foundations and Earth Structures. Design Manual*, Department of the Navy Facilities Engineering Command, Alexandria, USA.

Wong K.S. and Broms B.B. (1989). Lateral wall deflections of braced excavation in clay. *Journal of Geotechnical and Geoenvironmental Engineering*, 115(6), 853–870.

Wong K.S. and Goh A.T.C. (2002). Basal heave stability for wide excavations. *Proceeding of the Third International Conference of European Asian Civil Engineering Forum*, Aspects of Underground Construction in Soft Ground, Toulouse, 699-704.

Zienkiewicz O., Humpheson C., and Lewis R. (1975). Associated and non-associated visco-plasticity and plasticity in soil mechanics. *Geotechnique*, 25, 671–689.